TITLE: Voluntary co-contraction of ankle muscles alters motor unit discharge characteristics and reduces estimates of persistent inward currents

AUTHORS: Matheus M. Gomes[1,2*], Sophia T. Jenz[1*], James A. Beauchamp[1,3], Francesco Negro[4], C.J. Heckman[1], and Gregory E.P. Pearcey[1,5]

[1]Department of Physical Therapy and Human Movement Sciences, Feinberg School of Medicine, Northwestern University, Chicago, USA.

[2]School of Physical Education and Sport of Ribeirão Preto, University of São Paulo, Ribeirão Preto, Brazil.

[3]Department of Biomedical Engineering, McCormick School of Engineering, Northwestern University, Chicago, IL, USA

[4]Department of Clinical and Experimental Sciences, Universita degli Studi di Brescia, Brescia, Italy.

[5]School of Human Kinetics and Recreation, Memorial University of Newfoundland, St. John's, Canada.

* M.M. Gomes and S.T. Jenz contributed equally to this work.

Running title: Voluntary co-contraction reduces estimates of PICs

***Address for correspondence**:*

Matheus Gomes (mmgomes@usp.br) or Gregory Pearcey (gpearcey@mun.ca)

ABSTRACT

Motoneuronal persistent inward currents (PICs) are both facilitated by neuromodulatory inputs and highly sensitive to local inhibitory circuits (e.g., Ia reciprocal inhibition). Methods aimed to increase group Ia reciprocal inhibition from the antagonistic muscle have been successful in decreasing PICs, and the diffuse actions of neuromodulators released during activation of remote muscles have increased PICs. However, it remains unknown how motoneurons function in the presence of simultaneous excitatory and inhibitory commands. To probe this topic, we investigated motor unit (MU) discharge patterns and estimated PICs during voluntary co-contraction of ankle muscles, which simultaneously demands the contraction of agonist-antagonist pairs. Twenty young adults randomly performed triangular ramps (10s up and down) of both co-contraction (simultaneous dorsiflexion and plantarflexion) and isometric dorsiflexion to a peak of 30% of their maximum muscle activity from a maximal voluntary contraction. Motor unit spike trains were decomposed from high-density surface electromyography recorded over the tibialis anterior (TA) using blind source separation algorithms. Voluntary co-contraction altered motor unit discharge rate characteristics, decreasing estimates of PICs by 20% (4.47 pulses per second (pps) vs 5.57 pps during isometric dorsiflexion). These findings suggest that, during voluntary co-contraction, the inhibitory input from the antagonist muscle overcomes the additional excitatory and neuromodulatory drive that may occur due to the co-contraction of the antagonist muscle, which constrains PIC behavior.

KEY POINTS

Voluntary co-contraction is a unique motor behavior that concurrently provides increases in excitatory and inhibitory inputs to motoneurons.

During co-contraction of agonist-antagonist pairs, agonist motor unit discharge characteristics are altered, consistent with reductions in persistent inward current magnitude.

Reciprocal inhibition from the antagonist likely becomes proportional to the increase in neural drive to the agonist, dampening the magnitude of persistent inward currents.

INTRODUCTION

It is now well-established that monoaminergic inputs from the brainstem facilitate persistent inward currents (PICs), which modulate the excitability of the motor pool and are necessary for normal motor behavior (Heckman *et al.*, 2005; Heckman & Enoka, 2012; Johnson *et al.*, 2017). PICs are depolarizing currents generated by dendritic voltage sensitive ion channels that increase motoneuronal excitability by amplifying and prolonging synaptic inputs (Heckman *et al.*, 2005). The magnitude of PICs depends directly on the level of monoamines released, in particular norepinephrine (NE) and serotonin (5HT) (Lee & Heckman, 2000; Heckman *et al.*, 2005; Heckman & Enoka, 2012), but also the amount and pattern of inhibition from local circuits (Heckman *et al.*, 2009; Binder *et al.*, 2020).

The majority of evidence on the inhibitory control of PICs arises from animal studies and computer models (Hultborn *et al.*, 2003; Kuo *et al.*, 2003; Hyngstrom *et al.*, 2007; Bui *et al.*, 2008) but the magnitude of PICs in human motoneurons can be estimated quite easily due to recent advances in technology and analysis techniques (Klotz *et al.*, 2023; Möck & Del Vecchio, 2023). There remains a scarcity of research in humans, however, that establishes a relationship between reciprocal inhibition and PIC magnitude (Thorstensen, 2022). Mesquita et. al. (2022) recently found that stimulation of the common peroneal nerve, which induces reciprocal inhibition of the plantar flexors, can reduce PIC magnitude estimated from motor units decomposed from the human gastrocnemius and we have shown that vibration of an antagonist muscle tendon can reduce estimates of PIC magnitude, which we believe were due to reciprocal inhibition triggered by the vibratory stimuli of the antagonist muscles (Pearcey *et al.*, 2022). Since vibration is a crude method of inducing reciprocal inhibition, as it can induce several types of sensory input (e.g., non-locally mechanoreceptors, heteronomous muscle spindles) which may also impact motoneuron excitability, we remained interested in exploring further experimental paradigms that exemplify the control of PIC magnitude.

Examining the behavior of motor units of the agonist muscle during the voluntary muscle contraction of its antagonist (i.e., voluntary co-contraction) is a promising way to deepen understanding about the interplay between inhibitory control and neuromodulatory mechanisms underlying motor unit discharge characteristics. Contrary to most motor actions, where contraction of an agonist muscle causes reciprocal inhibition of its antagonistic pair, an isometric co-contraction task demands simultaneous contraction of antagonistic muscles and likely alters the structure of excitatory, inhibitory, and neuromodulatory commands to motoneurons.

Therefore, to understand the effect of voluntary muscle co-contraction on motor unit properties in humans, we compared motor unit discharge rate profiles during both isometric dorsiflexion and co-contraction tasks about the human ankle. Since PICs are highly sensitive to inhibition and voluntary co-contraction of the antagonist will likely impart reciprocal inhibition onto the agonist muscle, we hypothesized that co-contraction would alter motor unit discharge rate profiles, which would indicate lower PIC magnitude.

METHODS

Participants and Ethical Approval

Twenty healthy adults were recruited for this study. However, four participants were excluded because they were not able to perform the co-contraction task properly. Data from sixteen adults (7 Female; 30.3 ± 6.2 years) were analyzed. Participants had no experience with co-contraction training and no history of neuromuscular, musculoskeletal, or other abnormalities that would prevent them from completing the tasks described below. All participants provided written informed consent, approved by the Institutional Review Board of Northwestern University (STU00202964, STU00216332).

Experimental Protocol

Participants first performed three maximum voluntary isometric contractions (MVCs) of five seconds for each condition (i.e., dorsiflexion, plantarflexion, and co-contraction), with 90-second rest intervals between each attempt. If there was greater than 10% difference between MVC trials in peak torque (during dorsiflexion and plantarflexion) or rectified TA/SOL EMG amplitude (during co-contraction), additional trials were added. Verbal encouragement was given to participants during MVC trials to ensure maximal muscle contraction. The maximum torque and EMG amplitudes achieved during MVCs were used for subsequent normalization of all trials.

Participants next performed a familiarization comprised of 10 to 20 triangular-shaped ramps of TA contractions and co-contractions. The triangular ramp consisted of 10s linear ascending and descending phases to a peak of 30% of the rectified TA EMG achieved during maximal voluntary co-contraction. Participants received real-time visual feedback of the TA EMG during all submaximal ramp contractions on a large monitor that was positioned 2m away (Figure 1).

For the experimental protocol, participants performed four co-contraction ramps and four dorsiflexion ramps in a randomized order. Since co-contraction demands simultaneous activation of the plantar flexor and dorsiflexor muscles, we expected very little ankle torque. As such, if participants performed more than 20% of their maximum torque in either direction (dorsiflexion and plantarflexion) during co-contraction, additional trials were added as needed.

Torque recording

Isometric torque during dorsiflexion, plantarflexion, and co-contraction were collected using a Systems 2 isokinetic dynamometer (Biodex Medical System, Shirley, NY). Participants

were seated with their right foot in a footplate attachment, the hip in approximately 100º of flexion, knee at approximately 170º, and ankle at 100º (Figure 1). Velcro straps were wrapped around the foot to secure it to the plate and prevent movement. Torque was sampled at 2048 Hz and smoothed offline with a 10 Hz low-pass filter (fifth-order Butterworth filter).

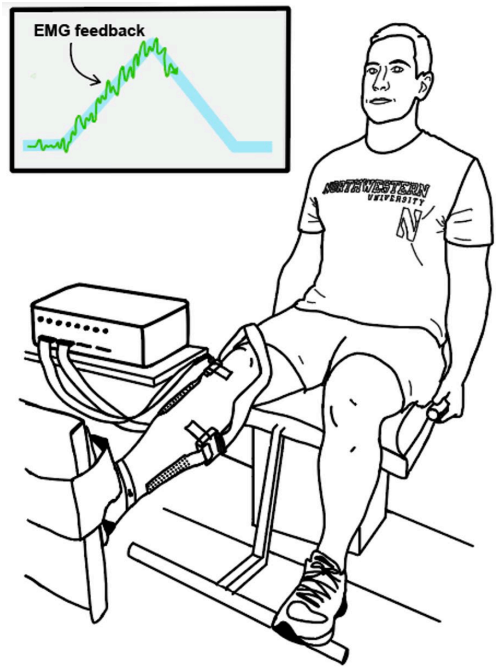

Figure 1 – Participant performing a co-contraction triangular ramp. The blue triangular trace represents the contraction intensity (target) to be performed and the green line represents a smoothed TA electromyogram visual feedback.

High-density surface electromyography (HD-sEMG) Recording

Before electrode placement, excess hair was removed and the skin overlying the muscle of interest was lightly abraded. High-density surface EMG (HD-sEMG) electrodes (64 electrodes, 13x5, 8mm I.E.D., GR08MM1305, OT Bioelettronica, Inc., Turin, IT) were placed longitudinally over the muscle belly of the tibialis anterior (TA) and soleus (SOL) (Rainoldi *et al.*, 2004), which are dorsiflexor and plantar flexor muscles of the ankle, respectively (Figure 1). A reference electrode strap was placed around the right ankle, overlying the medial and lateral malleolus. The HD-sEMG signals were collected in differential mode, sampled at 2048 Hz, amplified x150, and band-pass filtered at 10-500Hz using a Quattrocento signal amplifier (OT Bioelettronica, Inc., Turin, IT). EMG and torque were temporally synced with a 1-second TTL pulse transmitted to the Quattrocento at the onset of each trial. In order to provide EMG feedback to participants, the

signal from one channel of the TA electrode was amplified (x16) using OTbio+ software from the analog output feature. The EMG channel was chosen based on a central location on the electrode and signal to noise quality. This EMG channel was output to a NI DAQ (NI-USB-6218) where a custom MATLAB script was used to process and display the feedback onto the screen. The feedback EMG was lowpass filtered (1.8 Hz), the resting baseline was removed, and averaged over 60 ms intervals before being provided back to the participant.

Data Analysis

Torque: From the MVC trials, the maximum voluntary torque (MVT) achieved was used for subsequent normalization of all trials. Regarding the co-contraction ramp trials, only trials in which the participant did not achieve significant torque in any direction (i.e., less than 20% of the maximum dorsiflexion and plantarflexion torque) were included in subsequent analyses.

Motor unit decomposition: All surface HD-sEMG signals were initially bandpass filtered at 10–500 Hz (second-order, Butterworth) and visually inspected to remove substantial artifacts or noise. Individual motor unit spike trains were decomposed from the remaining HDsEMG channels using a convolutive blind-source separation algorithm with a silhouette threshold of 0.87 (Negro *et al.*, 2016). After decomposition, motor unit spike trains were manually edited by a trained technician. This inspection used a custom-made graphical user interface in MATLAB to correct minor errors made by the decomposition algorithm using well-validated local re-optimization methods to improve motor unit spike trains similar to the techniques used in recent studies(Boccia *et al.*, 2019; Afsharipour *et al.*, 2020; Del Vecchio *et al.*, 2020; Martinez-Valdes *et al.*, 2020; Jenz *et al.*, 2023). Instantaneous discharge rates of each motor unit spike train were determined by computing the inverse of the interspike interval and smoothed using support vector regression (Beauchamp *et al.*, 2022) with custom-written MATLAB scripts. Within these scripts, the initial, peak, and final discharge rates were extracted from the smoothed spike trains. Ascending duration was calculated as the time that a motor unit exhibited sustained discharge before peak torque, and descending duration as the time a motor unit exhibited sustained discharge from peak torque to derecruitment. Finally, recruitment threshold was calculated as the level of torque at the first motor unit spike.

Estimates of Persistent Inward Currents (PICs): Effects of PICs on motor unit discharge patterns can be estimated by quantifying the amount of onset-offset hysteresis (i.e., ΔFrequency, ΔF) of a higher-threshold (test) motor unit with respect to the discharge rate of a lower-threshold (reporter) unit (Gorassini et al. 1998, 2002). Rather than providing ΔF values for each test-reporter

unit pair, we calculated 'unit-wise' values, which gives each test unit one ΔF value based on the average values obtained from multiple reporter units. Criteria for inclusion of ΔF values from motor unit pairs were that 1) the test unit was recruited at least 1 second after the reporter unit to ensure full activation of the PIC (Bennett *et al.*, 2001; Powers *et al.*, 2008; Hassan *et al.*, 2020), 2) test unit-reporter unit pair exhibited rate-rate correlations ≥ 0.7 to ensure motor unit pairs received common synaptic drive (Gorassini *et al.*, 2004; Udina *et al.*, 2010; Stephenson & Maluf, 2011; Vandenberk & Kalmar, 2014), and 3) the reporter unit displayed a discharge range of at least 0.5 pps while the test unit was active (Stephenson & Maluf, 2011).

Geometric Analysis: We used an additional method, referred to as brace height (Beauchamp et al., 2023) to quantify the nonlinearity of motor unit discharge rate with respect to EMG output. Using the smoothed discharge rate of a single motor unit, we quantified the maximum orthogonal deviation between this smoothed discharge and an expected linear increase from motor unit recruitment to peak discharge, with the maximal deviation representing the "brace height". Brace height values were normalized to the height of a right triangle with a hypotenuse from recruitment to peak MU discharge. Motor units with a negative acceleration phase slope, brace height exceeding 200% after normalization, or peak discharge occurring after peak force were excluded. To distinguish between the secondary and tertiary phases of motor unit discharge, we calculated slopes for the initial acceleration phase and subsequent attenuation phase of motor unit discharge, along with the angle formed between these phases (Beauchamp et al., 2023).

***Tracking Motor Units*:** Motor units from isometric and co-contraction trials were tracked using a custom MATLAB script, which tracked motor units using blind source separation filters of the motor unit spike trains (Francic & Holobar, 2021; Oliveira & Negro, 2021; Goodlich *et al.*, 2023). The dataset of tracked motor units were analyzed using the same methods as the full dataset, and results are reported.

Statistical analysis

Statistical analyses were performed using R Statistical Software (v4.1.0; R Core Team 2021). To determine if the fixed effect of contraction type predicted variables of interest, we used linear mixed effects models (lmer R package; v1.1.27.1; (Bates *et al.*, 2015). To determine significance, we applied Satterthwaite's method for degrees of freedom (lmerTest R package; v3.1.3; (Kuznetsova *et al.*, 2017). Estimated marginal means and effect size (Cohen's *d*) were computed for each variable (emmeans R package, v1.8.0,(Lenth RV, Bolker B, Buerkner P, Gine-Vázquez I, Herve M & Love J, Miguez F, Riebl H, 2023). Results are reported as emmeans ±

206 standard deviation. Effect size was used to determine the effect of condition from the estimated
207 marginal means of isometric and co-contraction data from the model. All data were visualized in
208 R (ggplot R package, v3.3.6) (Wickham H, Chang W, Henry L, Pedersen TL, Takahashi K & Woo
209 K, Yutani H, Dunnington D, 2023)

210

RESULTS

EMG and Torque During Isometric and Co-contraction

To evaluate how effectively participants performed the challenging co-contraction task, we compared net ankle torque and EMGs in both the agonist and antagonist between the isometric and co-contraction protocols. The peak dorsiflexion torque was much higher in the isometric condition (43.1 ± 2.90 %MVT) than during co-contraction (14.0 ± 2.91 %MVT $\chi^2_{(1)} = 162.57$, $P < 0.001$, $d = 3.67$). Peak agonist (TA) EMG did not differ during isometric (26.0 ± 1.13 %MVEMG) or co-contraction (26.9 ± 1.14 %MVEMG; $\chi^2_{(1)} = 1.1634$, $P = 0.281$, $d = -0.20$). However, the peak EMG of the antagonist muscle (SOL) was much lower during isometric (6.7 ± 1.62 %MVEMG) than co-contraction (12.2 ± 1.64 %MVEMG; $\chi^2_{(1)} = 17.15$, $P < 0.001$, $d = -0.803$). The similarity in TA EMG magnitude during both contractions allows for the comparison of motor units between the two conditions.

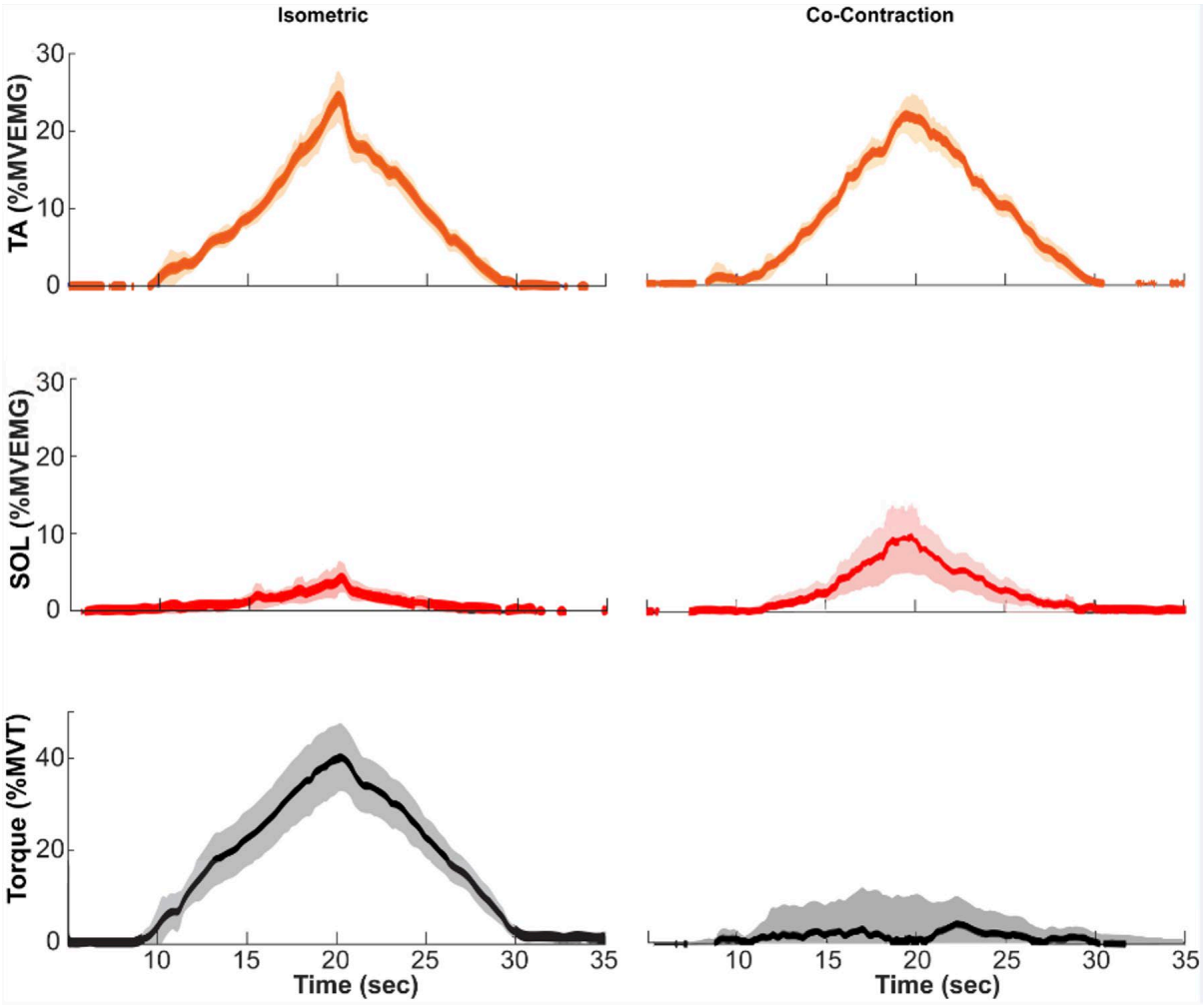

Figure 2 – Normalized EMG torque and dorsiflexion torque during isometric and co-contraction shows participants correctly performed co-contraction. Normalized EMG for the agonist muscle, TA, is shown in orange and antagonist, SOL, in red. Normalized dorsiflexion torque is shown in black. Abbreviations: MVEMG; maximal voluntary EMG; MVT; maximal voluntary torque.

Motor units decomposed (per trial and participant for each condition) and recruitment torques

Across all the trials, 1,031 units were decomposed from the isometric condition and 996 units were decomposed from the co-contraction condition. Participants had more difficulty performing co-contraction successfully, and therefore there were fewer valid attempts (trials) at co-contraction. On average 16.60 units were decomposed per trial for the isometric condition, and 17.47 units per trial for the co-contraction condition. Figure 3 shows the distribution of motor unit recruitment was similar in isometric and co-contraction.

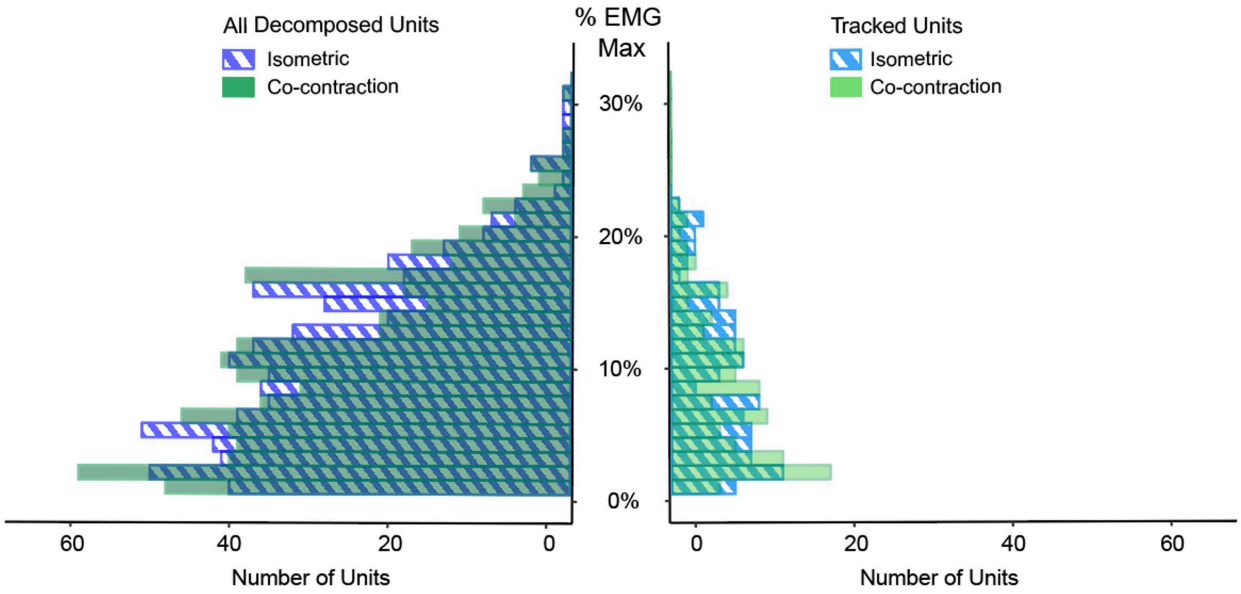

Figure 3 – The number of motor units decomposed by %EMG recruited for the full and tracked datasets for isometric (blue hatched) and co-contraction (solid green) conditions.

Motor Unit Discharge Rate Differs between Conditions

To gain insight into motor unit activity during the triangular ramps we quantified discharge rate at recruitment, derecruitment, and the peak discharge rate (Table 1). In the full dataset, the motor unit discharge rate at recruitment was higher during the isometric condition ($\chi^2_{(1)}$ = 15.135, $P < 0.001$, $d = 0.22$), but the discharge rate at derecruitment was lower in isometric ($\chi^2_{(1)}$ = 4.1794, $P = 0.041$, $d = -0.115$). Peak discharge rate was higher during co-contraction ($\chi^2_{(1)}$ = 10.16, $P = 0.001$, $d = -0.19$). For tracked MUs, discharge rate was similar at recruitment ($\chi^2_{(1)}$ = 1.374, $P < 0.241$, $d = 0.142$) and peak ($\chi^2_{(1)}$ = 2.122, $P = 0.145$, $d = -0.177$), but was lower in isometric at derecruitment ($\chi^2_{(1)}$ = 4.805, $P < 0.028$, $d = -0.268$). These values show motor unit discharge of the agonist muscle is altered when the antagonist is simultaneously active (Figure 4).

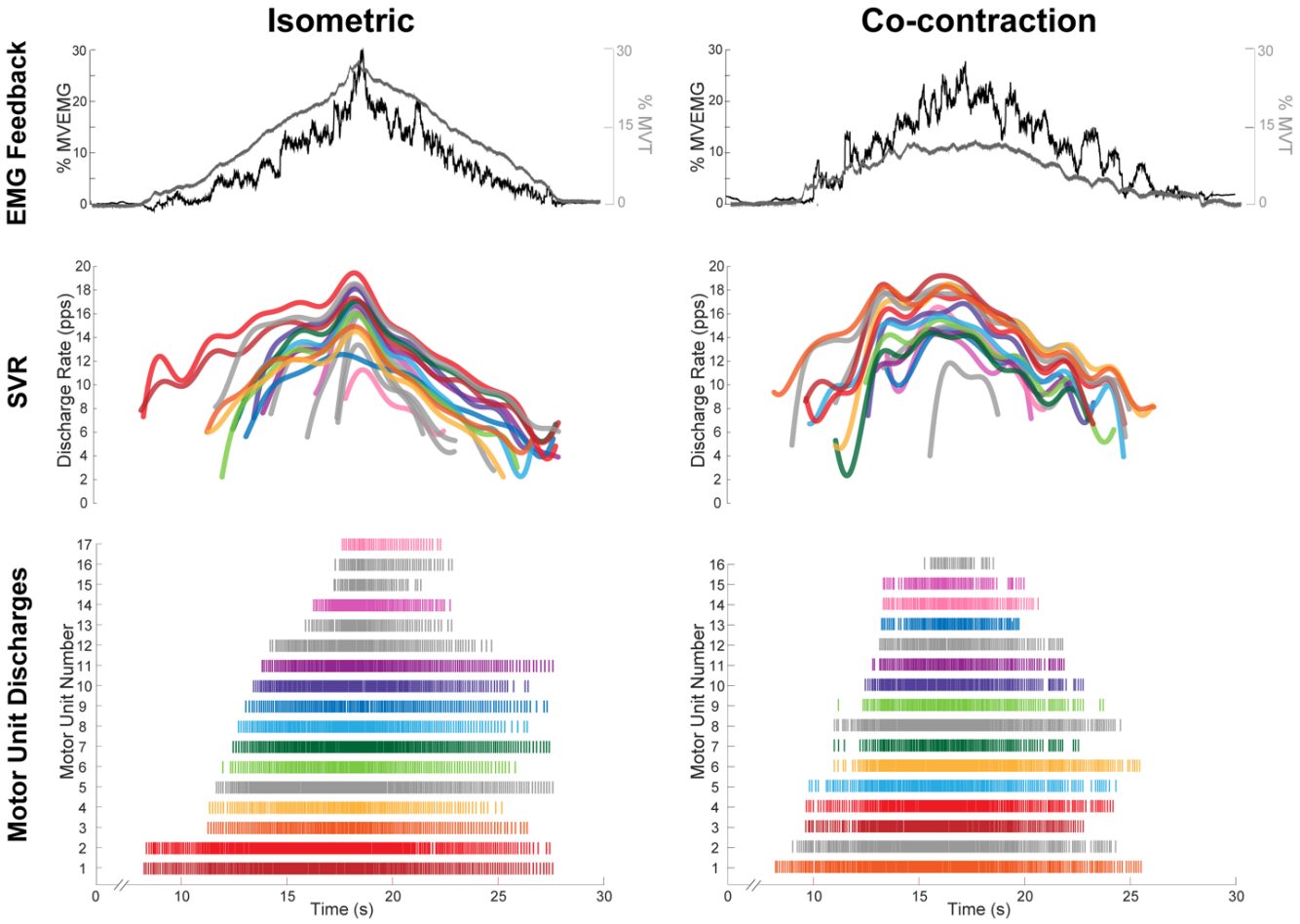

Figure 4 – Example of a single isometric and co-contraction trial from one participant. EMG feedback (black) and dorsiflexion torque (gray) are shown on the top trace. Smoothed

motor units with a support vector regression (SVR) are shown in the middle. At the bottom are raster plots showing the individual discharge patterns of units. Units that were matched between the two trials are color coded, and those with no matches are shown in grey.

Table 1. Motor unit discharge rates during triangular ramp contractions. Estimated marginal means and standard errors are shown for isometric and co-contraction conditions, with all motor units on the left and tracked motor units on the right. Abbreviations: pps; pulses per second; SE; standard error. Significance noted as: '*' *P* < 0.001, '**' *P* < 0.01, '*' *P* < 0.05.**

A. DISCHARGE RATE AT RECRUITMENT

	All Data		*Tracked Data*	
	Mean (pps)	*SE*	*Mean (pps)*	*SE*
ISOMETRIC	*9.35****	0.390	8.62	0.40
CO-CONTRACTION	*8.75****	0.391	8.26	0.40

B. PEAK DISCHARGE RATE

	All Data		*Tracked Data*	
	Mean (pps)	*SE*	*Mean (pps)*	*SE*
ISOMETRIC	*15.70****	0.668	16.9	0.52
CO-CONTRACTION	*16.00****	0.667	17.2	0.52

C. DISCHARGE RATE AT DERECRUITMENT

	All Data		*Tracked Data*	
	Mean (pps)	*SE*	*Mean (pps)*	*SE*
ISOMETRIC	*6.84**	0.243	6.41*	0.314
CO-CONTRACTION	*7.08**	0.243	6.97*	0.314

Motor Unit Discharge Duration Differs between Conditions

To gain additional insight about the timing of discharge in relation to the triangular target that participants were given, we quantified the duration of motor unit discharge (Table 2). In the full

dataset ascending phase duration was higher in isometric contractions ($\chi^2_{(1)}$ = 11.457, P < 0.001, d = 0.246). Descending phase duration was higher during co-contraction ($\chi^2_{(1)}$ = 7.8472, P = 0.005, d = -0.163) and the ascending-descending phase ratio was larger during co-contraction ($\chi^2_{(1)}$ = 17.026, P < 0.001, d = 0.24). For tracked MUs, ascending phase duration was higher during isometric ($\chi^2_{(1)}$ = 5.908, P < 0.015, d = 0.296), but descending phase duration was similar between conditions ($\chi^2_{(1)}$ = 1.792, P < 0.181, d = -0.164). The ascending-descending phase ratio was also similar between conditions in the tracked data ($\chi^2_{(1)}$ = 1.107, P = 0.293, d = 0.128).

Table 2. Motor unit discharge rates duration during triangular ramp contractions. Estimated marginal means and standard errors are shown for isometric and co-contraction conditions, with all motor units on the left and tracked motor units on the right. Abbreviations: sec; seconds; SE; standard error. Significance noted as: '*' *P* < 0.001, '**' *P* < 0.01, '*' *P* < 0.05.**

A. ASCENDING PHASE DURATION

	All Data		*Tracked Data*	
	Mean (sec)	*SE*	*Mean (sec)*	*SE*
ISOMETRIC	*5.61****	0.219	6.15*	0.201
CO-CONTRACTION	*5.34****	0.218	5.82*	0.202

B. DESCENDING PHASE DURATION

	All Data		*Tracked Data*	
	Mean (sec)	*SE*	*Mean (sec)*	*SE*
ISOMETRIC	*6.86***	0.235	6.93	0.251
CO-CONTRACTION	*7.15***	0.234	7.11	0.251

C. ASCENDING-DESCENDING PHASE RATIO

	All Data		*Tracked Data*	
	Mean (sec)	*SE*	*Mean (sec)*	*SE*
ISOMETRIC	*-0.121****	0.0308	-0.102	0.029
CO-CONTRACTION	*-0.174****	0.0305	-0.124	0.029

To identify a mechanism responsible for different discharge patterns in the two conditions we estimated PIC magnitude. Estimates of PICs (ΔF) were higher in the isometric condition, in both

the full dataset ($\chi^2_{(1)}$ = 72.663, P < 0.001, d = 0.641) and the tracked units ($\chi^2_{(1)}$ = 14.597, P < 0.001, d = 0.656; Figure 5A).

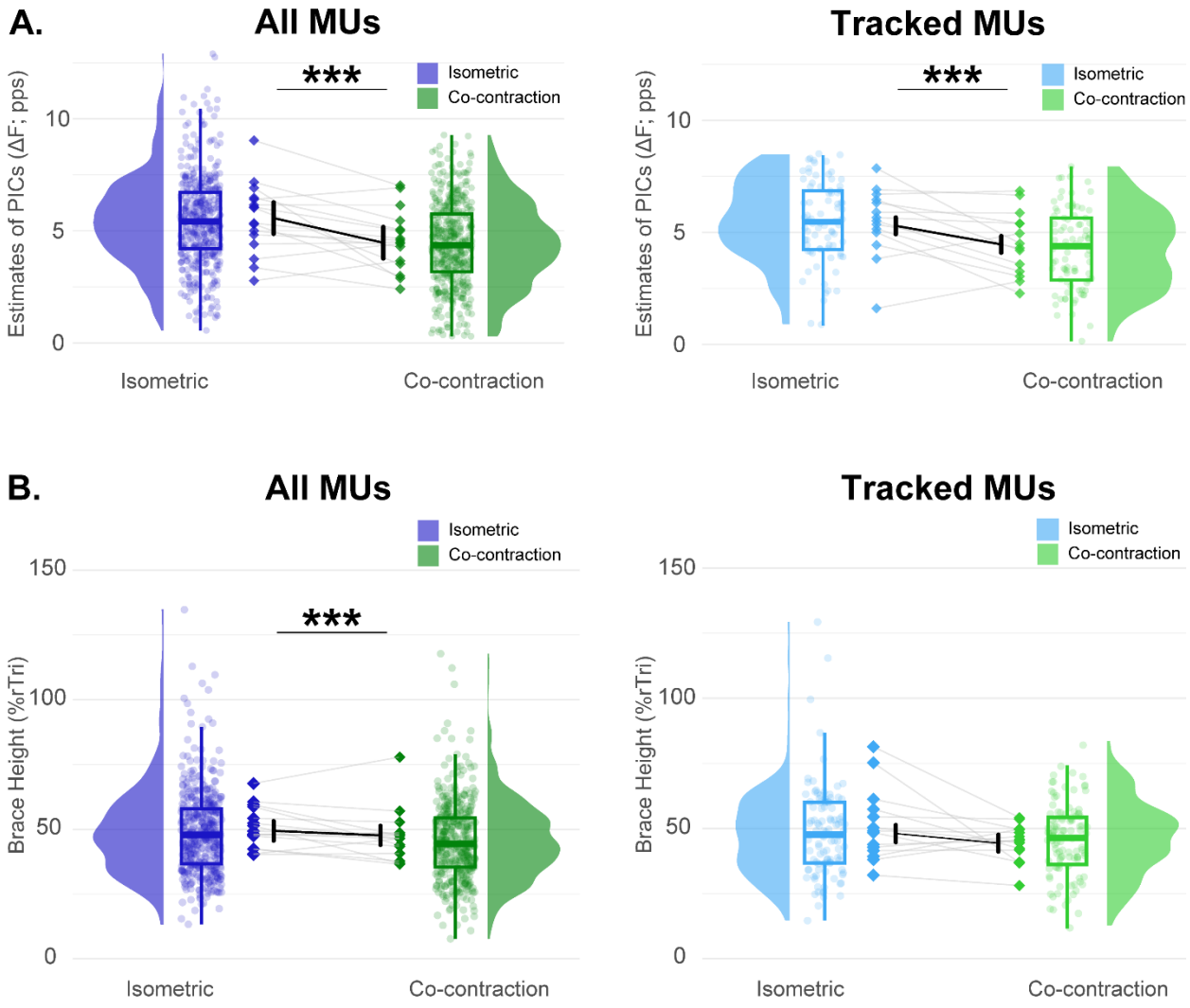

Figure 5 – Estimates of persistent inward currents (top) and brace height (bottom) from the tibialis anterior during isometric (blue) and co-contraction (green). The entire dataset is shown to the right of each plot and the tracked dataset is shown to the left. Model estimates are shown in the dark black lines, individual participant means are shown as diamonds. Box plots show the 25th, 50th(median), and 75th quartiles, with whiskers showing the 1.5 interquartile range. Distributions across all participants of the respective measure are shown. Significance noted as: '*' P < 0.001, '**' P < 0.01, '*' P < 0.05.**

To further probe potential differences in the pattern of inhibition and neuromodulatory to the motoneuron pool during the two tasks, we utilized a quasi-geometric analysis of the individual motor unit discharge rate profiles with respect to the EMG feedback that participants received. Brace height was higher in the isometric condition than co-contraction for the full data ($\chi^2_{(1)}$ = 19.655, P < 0.001, d = 0.254) and, although the model did not indicate significant differences, trended higher in the tracked dataset ($\chi^2_{(1)}$ = 3.8287, P = 0.0503, d = 0.283; Figure 5A). The acceleration and attenuation slopes did not differ between conditions in both the full (ACC $\chi^2_{(1)}$ = 2.73, P = 0.098, d = 0.126; ATT $\chi^2_{(1)}$ = 0.226, P = 0.634, d = 0.034) and tracked (ACC $\chi^2_{(1)}$ = 0.195, P = 0.659, d = -0. 0612; ATT $\chi^2_{(1)}$ = 0.454, P = 0.501, d = -0.098) datasets. The angle between the acceleration and attenuation phases was greater during isometric than co-contraction (ANG $\chi^2_{(1)}$ = 18.117, P < 0.001, d = 0.34) but similar between conditions in the tracked units (ANG $\chi^2_{(1)}$ = 0.151, P = 0.698, d = 0.056).

Finally, to gain insight about whether there were shifts in the recruitment threshold of motor units, we assessed the amplitude of EMG where the motor unit was recruited. Motor unit recruitment EMG was similar between conditions in the full ($\chi^2_{(1)}$ = 0.0008, P = 0.978, d = -0.003) but was higher for isometric contractions of the tracked datasets ($\chi^2_{(1)}$ = 11.228, P = 0.001, d = 0.412; Table 3). This indicates that the recruitment thresholds (in terms of agonist EMG) were reduced during co-contraction.

Table 3. Geometric metrics and recruitment electromyogram amplitude during triangular ramp contractions. Estimated marginal means and standard errors are shown for isometric and co-contraction conditions, with all motor units on the left and tracked motor units on the right. Abbreviations: pps; pulses per second; SE; standard error; Tri; triangle; %MEMG; percentage maximum EMG. Significance noted as: '*' P < 0.001, '**' P < 0.01, '*' P <0.05.**

A. ACCELERATION SLOPE

	All Data		*Tracked Data*	
	Mean (pps/ %MEMG)	*SE*	*Mean (pps/ %MEMG)*	*SE*
ISOMETRIC	*1.41*	0.078	1.55	0.227
CO-CONTRACTION	*1.25*	0.079	1.68	0.222

B. ATTENUATION SLOPE

	All Data	*Tracked Data*

	Mean (pps/ %MEMG)	*SE*	*Mean (pps/ %MEMG)*	*SE*
ISOMETRIC	*0.252*	0.0184	*0.267*	0.0358
CO-CONTRACTION	*0.245*	0.0180	*0.289*	0.0356

C. ANGLE

	All Data		*Tracked Data*	
	Mean (degrees)	*SE*	*Mean (degrees)*	*SE*
ISOMETRIC	*237****	2.96	231	3.07
CO-CONTRACTION	*229****	2.95	230	3.05

D. MOTOR UNIT RECRUITMENT EMG

	All Data		*Tracked Data*	
	Mean (%MEMG)	*SE*	*Mean (%MEMG)*	*SE*
ISOMETRIC	*9.33*	0.405	8.68***	0.501
CO-CONTRACTION	*9.35*	0.408	7.57***	0.501

DISCUSSION

The purpose of this study was to investigate the effects of intentional muscle co-contraction on TA motor unit discharge patterns during submaximal isometric ramp contractions in the lower limb. Our results revealed that voluntary antagonist co-contraction affected motor unit discharge patterns, which reduced estimates of persistent inward currents (ΔF). The novel findings from this study add to our basic understanding of how the interplay between excitatory, inhibitory, and neuromodulatory motor commands shape motor unit discharge rate profiles.

EMG and torque during isometric and co-contraction

Voluntary co-contraction is a complex task due to the competing activation of antagonist pairs that likely impart inhibition onto each other (i.e., reciprocal inhibition) (Crone *et al.*, 1987; Hirabayashi *et al.*, 2019). Successful execution requires highly complex commands to compensate for the additional inhibition that is not present during traditional contraction (i.e., only involving the agonist muscle). Increasing and decreasing the intensity of co-contraction, as done in the triangular ramp used in the present study, made the task even more challenging. In fact, four participants were excluded from the sample because of their inability to perform the co-contraction ramp with linear increases and decreases in EMG amplitude without increasing torque about the ankle. Among these participants, some contracted one muscle (e.g., TA) more than the other muscle in the antagonist pair (e.g., SOL), resulting in torque generation at the ankle. Meanwhile, others were unable to gradually contract both sets of antagonist muscles to reach the target intensity. Sixteen participants performed the co-contraction ramp appropriately, as evidenced by similar TA EMG, greater soleus EMG, and minimal torque compared to the dorsiflexion isometric condition (Figure 2).

Motor unit discharge rates differ between conditions

While the TA EMG activity was similar between conditions (i.e., dorsiflexion and co-contraction), the motor unit discharge characteristics differed. It is well established that the volitional activation of an agonist muscle generates Ia afferent input that, through intraspinal circuits, inhibits its antagonist pair (i.e., reciprocal inhibition) (Crone *et al.*, 1987; Hirabayashi *et al.*, 2019). Therefore, it is reasonable to consider that during co-contraction the simultaneous contraction of antagonist muscles (i.e., plantarflexor muscles) would induce inhibition that would interfere with agonist motor unit discharge (i.e., TA muscle). During co-contraction, the motor unit discharge rate at recruitment was lower, while the peak discharge rate and the discharge rate at derecruitment were higher compared to isometric dorsiflexion. Previous studies that applied

vibratory stimuli to the plantarflexor muscles also observed alterations in TA discharge rate characteristics and suggested that these changes were induced by the reciprocal inhibition mechanism (Mesquita *et al.*, 2022; Pearcey *et al.*, 2022; Orssatto *et al.*, 2022). Even though we acknowledge that reciprocal inhibition is a factor influencing motor unit discharge rates, the changes we observed diverge from those reported in previous studies. Here we observed a reduction in the discharge rate at recruitment in the condition that induces reciprocal inhibition (i.e., co-contraction), whereas previously we (Pearcey *et al.*, 2022) observed an increase with antagonist vibration. Similarly, while we observed an increase in peak discharge rate and discharge rate at derecruitment in the condition affected by reciprocal inhibition (i.e., co-contraction), previous studies reported an increase in discharge rate when reciprocal inhibition was present (Mesquita *et al.*, 2022; Pearcey *et al.*, 2022; Orssatto *et al.*, 2022). Reciprocal inhibition in these previous studies was induced by antagonist nerve stimulation (Mesquita *et al.*, 2022) or antagonist tendon vibration (Pearcey *et al.*, 2022; Orssatto *et al.*, 2022), whereas currently reciprocal inhibition was induced by the voluntary co-contraction of the antagonist muscle. It has been demonstrated that contraction of remote muscle groups can amplify motoneuron excitability, probably through increased monoamines delivered by descending tracts from the brainstem (Heckman *et al.*, 2008; Wei *et al.*, 2014; Orssatto *et al.*, 2022). Thus, the voluntary co-contraction of the antagonist muscle may have not only caused reciprocal inhibition but also increased the excitatory and neuromodulatory commands to the motoneurons.

Estimates of PICs were lower during co-contraction

Since PICs are highly sensitive to inhibition, reciprocal inhibition from contraction of antagonist pairs could reduce PICs in the agonist muscle. However, contracting remote muscle groups can increase PICs (Heckman *et al.*, 2008; Wei *et al.*, 2014; Orssatto *et al.*, 2022), and thus antagonist muscle contraction could increase monoaminergic drive and facilitate PICs during the co-contraction task. Here, we analyzed the combined effect of these two potential alterations in motor commands and find that local inhibition from antagonist muscle contraction appears to overcome any potential increase in neuromodulatory drive.

Our findings corroborate previous studies that have also observed a PIC reduction in the presence of reciprocal (Mesquita *et al.*, 2022; Pearcey *et al.*, 2022; Orssatto *et al.*, 2022). As mentioned above, these previous studies relied on methods to induce sensory input rather than direct activation of the antagonist muscle (Mesquita *et al.*, 2022; Pearcey *et al.*, 2022; Orssatto *et al.*, 2022). It is probable that these methods do not elicit the same monoaminergic input as the voluntary contraction of the antagonist muscle, which was specifically investigated in our study.

In this regard, our results complement the findings of Orssatto et. al. (2022) showing that the reciprocal inhibition input overlaps the increased monoaminergic drive triggered by the voluntary activation of the antagonist muscle. Furthermore, vibration applied to the antagonistic muscle can activate additional sensory inputs, such as non-local mechanoreceptors or heteronomous muscle spindles, which can influence the excitability of motoneurons (Garnett & Stephens, 1981; Barss *et al.*, 2021). Nevertheless, our results revealed that reciprocal inhibition induced by voluntary antagonist contraction elicited a similar reduction in ΔF (i.e. 1.1 pps, 19.7%) to those observed in the previous studies (Pearcey *et al.*, 2022; Orssatto *et al.*, 2022) that used vibratory stimuli (0.54 pps, 14.4%; 0.72 pps, 14.7%, respectively).

In summary, our results demonstrate that voluntary co-contraction represents an intriguing paradigm to facilitate the concurrent assessment of excitatory, neuromodulatory, and inhibitory inputs. Co-contraction elicits reciprocal inhibition and increased neuromodulatory input, which results in decreased PICs and alterations in the discharge rate profiles of motor units. Given that co-contraction has been employed as a resistance training method, forthcoming studies could explore whether prolonged co-contraction training induces enduring adaptations in the intrinsic properties of motor units.

METHODOLOGICAL CONSIDERATIONS

Due to the difficulty in performing the task, we assessed only one submaximal level of contraction (i.e., 30% MVC). Since contraction intensity has profound effects on the composition of motor commands (Škarabot *et al.*, 2023) future investigations with higher intensity co-contractions are needed to verify whether the reciprocal inhibition input will continue to overcome the increased monoaminergic drive resulting from the voluntary activation of the antagonist muscle. Another limitation is that we only analyzed the isometric condition in a single ankle position (i.e., at 100º). Alterations in the ankle angle can modify passive and active joint moments (Jamwal *et al.*, 2017), contractile properties of the muscles (i.e., tension-length relationship) (Rassier *et al.*, 1999; Cadeo *et al.*, 2023) and, in particular, motor unit discharge rate profiles and estimates of PICs(Beauchamp *et al.*, 2023*b*). Thus, a different ankle position could influence the recruitment threshold and discharge rate of the motor units required to maintain zero torque at the ankle during voluntary co-contraction. We also only assessed estimates of PICs and discharge rate patterns from the TA. It is important to consider that various muscles have diverse innervation (Banks, 2006; Kissane *et al.*, 2023), which may affect the extent of reciprocal inhibition. Finally, there were discrepancies in our findings when analyzing all motor units

compared to analyzing only tracked motor units. This likely is due to a lower sample size of tracked motor units across tasks, or could be due to a difference in recruitment threshold between the two conditions of the tracked motor units.

PRACTICAL APPLICATIONS

In the last decade, voluntary co-contraction has been proposed as a method of strength training. To do this, a person perform sets of voluntary simultaneous contraction (i.e., co-contraction) of antagonistic pairs (e. g. elbow flexors and extensors) with no external apparatuses for loading (Mackenzie *et al.*, 2010; Zbidi *et al.*, 2017; Fujita *et al.*, 2021). Previous studies have indicated that co-contraction training promotes strength gain (Mackenzie *et al.*, 2010; Villalba *et al.*, 2024) and hypertrophy (Counts *et al.*, 2016), similar to conventional resistance training, which makes this method very promising with potential application in microgravity and rehabilitation backgrounds. It is now apparent that the neural commands required to perform co-contraction differ from those to perform agonist contractions. These novel insights are likely to shed light on the application of these types of muscle contraction for adaptations in both health and disease.

CONCLUSION

Voluntary antagonist co-contraction significantly altered motor unit discharge characteristics and reduced estimates of persistent inward currents. The novelty of our approach, which concurrently considers both inhibitory and excitatory inputs arising from voluntary antagonist co-contraction, enhances our basic understanding of the interplay between excitatory, inhibitory, and neuromodulatory motor commands that shape motor unit discharge rate profiles. These findings also hold promise for optimizing therapeutic strategies and training protocols that utilize voluntary muscle co-contraction.

Data availability statement

The data that support the findings of this study are available on request from the corresponding author.

Competing interests

The authors declare that they have no competing interests.

Author contributions

M.M.G., S.T.J., J.A.B., C.J.H., and G.E.P.P. conceptualized and designed the research; M.M.G., S.T.J., J.A.B., and G.E.P.P performed the experiments; F.N developed blind source separation algorithms; M.M.G., S.T.J., and J.A.B. analyzed the data; M.M.G., S.T.J., J.A.B., C.J.H., and G.E.P.P. interpreted the results of experiments; M.M.G., S.T.J., and J.A.B. prepared the figures; M.M.G. and S.T.J. drafted the manuscript; M.M.G., S.T.J., J.A.B., F.N., C.J.H., and G.E.P.P. revised and approved the final version of the manuscript.

Funding

This work was supported by the São Paulo Research Foundation (FAPESP; grant #2020/03282-0), the National Institute of Health (NIH; grants R01NS098509-01, R01NS098509-05, and NINDS F31 NS120500), and the Natural Sciences and Engineering Research Council of Canada (NSERC; Discovery Grant 2023-05862, and Discovery Launch Supplement 2023-00279).

References

Afsharipour B, Manzur N, Duchcherer J, Fenrich KF, Thompson CK, Negro F, Quinlan KA, Bennett DJ & Gorassini MA (2020). Estimation of self-sustained activity produced by persistent inward currents using firing rate profiles of multiple motor units in humans. *J Neurophysiol* **124,** 63–85.

Banks RW (2006). An allometric analysis of the number of muscle spindles in mammalian skeletal muscles. *J Anat* **208,** 753–768.

Barss TS, Collins DF, Miller D & Pujari AN (2021). Indirect Vibration of the Upper Limbs Alters Transmission Along Spinal but Not Corticospinal Pathways. *Front Hum Neurosci*; DOI: 10.3389/FNHUM.2021.617669.

Bates D, Mächler M, Bolker BM & Walker SC (2015). Fitting linear mixed-effects models using lme4. *J Stat Softw*; DOI: 10.18637/jss.v067.i01.

Beauchamp JA, Khurram OU, Dewald JPA, Heckman CJ & Pearcey GEP (2022). A computational approach for generating continuous estimates of motor unit discharge rates and visualizing population discharge characteristics. *J Neural Eng*; DOI: 10.1088/1741-2552/AC4594.

Beauchamp JA, Pearcey GEP, Khurram OU, Chardon M, Wang YC, Powers RK, Dewald JPA & Heckman CJ (2023*a*). A geometric approach to quantifying the neuromodulatory effects of persistent inward currents on individual motor unit discharge patterns. *J Neural Eng*; DOI: 10.1088/1741-2552/ACB1D7.

Beauchamp JA, Pearcey GEP, Khurram OU, Negro F, Dewald JPA & Heckman C (2023*b*). Intrinsic properties of spinal motoneurons degrade ankle torque control in humans. *bioRxiv*2023.10.23.563670.

Bennett DJ, Li Y & Siu M (2001). Plateau potentials in sacrocaudal motoneurons of chronic spinal rats, recorded in vitro. *J Neurophysiol* **86,** 1955–1971.

Binder MD, Powers RK & Heckman CJ (2020). Nonlinear Input-Output Functions of Motoneurons. *Physiology (Bethesda)* **35,** 31–39.

Boccia G, Martinez-Valdes E, Negro F, Rainoldi A & Falla D (2019). Motor unit discharge rate and the estimated synaptic input to the vasti muscles is higher in open compared with closed kinetic chain exercise. *J Appl Physiol* **127,** 950–958.

Bui T V., Grande G & Rose PK (2008). Relative location of inhibitory synapses and persistent inward currents determines the magnitude and mode of synaptic amplification in motoneurons. *J Neurophysiol* **99,** 583–594.

Cadeo GM, Fujita RA, Villalba MM, Silva NRS, Júnior CI, Pearcey GEP & Gomes MM (2023). Myoelectric activity and improvements in strength and hypertrophy are unaffected by the ankle position during prone leg curl exercise - a within person randomized trial. *Eur J Sport Sci*; DOI: 10.1080/17461391.2023.2214794.

Counts BR, Buckner SL, Dankel SJ, Jessee MB, Mattocks KT, Mouser JG, Laurentino GC & Loenneke JP (2016). The acute and chronic effects of “NO LOAD” resistance training. *Physiol Behav* **164,** 345–352.

Crone C, Hultborn H, Jespersen B & Nielsen J (1987). Reciprocal Ia inhibition between ankle

flexors and extensors in man. *J Physiol* **389,** 163–185.

Francic A & Holobar A (2021). On the Reuse of Motor Unit Filters in High Density Surface Electromyograms Recorded at Different Contraction Levels. *IEEE Access* **9,** 115227–115236.

Fujita RA, Villalba MM, Silva NRS, Pacheco MM & Gomes MM (2021). Mind-Muscle Connection: Verbal Instructions Alter Electromyographic Activity for Elbow Flexors and Extensors During Co-Contraction Training. *Percept Mot Skills* **128,** 375–389.

Garnett R & Stephens JA (1981). Changes in the recruitment threshold of motor units produced by cutaneous stimulation in man. *J Physiol* **311,** 463–473.

Goodlich BI, Del Vecchio A & Kavanagh JJ (2023). Motor unit tracking using blind source separation filters and waveform cross-correlations: reliability under physiological and pharmacological conditions. *J Appl Physiol* **135,** 362–374.

Gorassini M, Yang JF, Siu M & Bennett DJ (2002). Intrinsic activation of human motoneurons: possible contribution to motor unit excitation. *J Neurophysiol* **87,** 1850–1858.

Gorassini MA, Knash ME, Harvey PJ, Bennett DJ & Yang JF (2004). Role of motoneurons in the generation of muscle spasms after spinal cord injury. *Brain* **127,** 2247–2258.

Hassan A, Thompson CK, Negro F, Cummings M, Powers RK, Heckman CJ, Dewald JPA & McPherson LM (2020). Impact of parameter selection on estimates of motoneuron excitability using paired motor unit analysis. *J Neural Eng*; DOI: 10.1088/1741-2552/AB5EDA.

Heckman CJ & Enoka RM (2012). Motor unit. *Compr Physiol* **2,** 2629–2682.

Heckman CJ, Gorassini MA & Bennett DJ (2005). Persistent inward currents in motoneuron dendrites: Implications for motor output. *Muscle and Nerve* **31,** 135–156.

Heckman CJ, Hyngstrom AS & Johnson MD (2008). Active properties of motoneurone dendrites: diffuse descending neuromodulation, focused local inhibition. *J Physiol* **586,** 1225–1231.

Heckman CJ, Mottram C, Quinlan K, Theiss R & Schuster J (2009). Motoneuron excitability: the importance of neuromodulatory inputs. *Clin Neurophysiol* **120,** 2040–2054.

Hirabayashi R, Edama M, Kojima S, Nakamura M, Ito W, Nakamura E, Kikumoto T & Onishi H (2019). Effects of Reciprocal Ia Inhibition on Contraction Intensity of Co-contraction. *Front Hum Neurosci*; DOI: 10.3389/FNHUM.2018.00527.

Hultborn H, Denton ME, Wienecke J & Nielsen JB (2003). Variable amplification of synaptic input to cat spinal motoneurones by dendritic persistent inward current. *J Physiol* **552,** 945–952.

Hyngstrom AS, Johnson MD, Miller JF & Heckman CJ (2007). Intrinsic electrical properties of spinal motoneurons vary with joint angle. *Nat Neurosci* **10,** 363–369.

Jamwal PK, Hussain S, Tsoi YH, Ghayesh MH & Xie SQ (2017). Musculoskeletal modelling of human ankle complex: Estimation of ankle joint moments. *Clin Biomech (Bristol, Avon)* **44,** 75–82.

Jenz ST, Beauchamp JA, Gomes MM, Negro F, Heckman CJ & Pearcey GEP (2023). Estimates of persistent inward currents in lower limb motoneurons are larger in females

549 than in males. *J Neurophysiol* **129,** 1322–1333.

550 Johnson MD, Thompson CK, Tysseling VM, Powers RK & Heckman CJ (2017). The potential
551 for understanding the synaptic organization of human motor commands via the firing
552 patterns of motoneurons. *J Neurophysiol* **118,** 520–531.

553 Kissane RWP, Charles JP, Banks RW & Bates KT (2023). The association between muscle
554 architecture and muscle spindle abundance. *Sci Rep*; DOI: 10.1038/S41598-023-30044-W.

555 Klotz T, Lehmann L, Negro F & Röhrle O (2023). High-density magnetomyography is superior to
556 high-density surface electromyography for motor unit decomposition: a simulation study. *J*
557 *Neural Eng*; DOI: 10.1088/1741-2552/ACE7F7.

558 Kuo JJ, Lee RH, Johnson MD, Heckman HM & Heckman CJ (2003). Active Dendritic Integration
559 of Inhibitory Synaptic Inputs in Vivo. *J Neurophysiol* **90,** 3617–3624.

560 Kuznetsova A, Brockhoff PB & Christensen RHB (2017). lmerTest Package: Tests in Linear
561 Mixed Effects Models. *J Stat Softw* **82,** 1–26.

562 Lee RH & Heckman CJ (2000). Adjustable amplification of synaptic input in the dendrites of
563 spinal motoneurons in vivo. *J Neurosci* **20,** 6734–6740.

564 Lenth RV, Bolker B, Buerkner P, Gin_e-Vázquez I, Herve M JM & Love J, Miguez F, Riebl H SH
565 (2023). emmeans: estimated marginal means, aka least-squares means (Online).

566 Mackenzie SJ, Rannelli LA & Yurchevich JJ (2010). *NEUROMUSCULAR ADAPTATIONS*
567 *FOLLOWING ANTAGONIST RESISTED TRAINING*. Available at:
568 http://www.ncbi.nlm.nih.gov/pubmed/19996784 [Accessed February 20, 2020].

569 Martinez-Valdes E, Negro F, Falla D, Dideriksen JL, Heckman CJ & Farina D (2020). Inability to
570 increase the neural drive to muscle is associated with task failure during submaximal
571 contractions. *J Neurophysiol* **124,** 1110–1121.

572 Mesquita RNO, Taylor JL, Trajano GS, Škarabot J, Holobar A, Gonçalves BAM & Blazevich AJ
573 (2022). Effects of reciprocal inhibition and whole-body relaxation on persistent inward
574 currents estimated by two different methods. *J Physiol* **600,** 2765–2787.

575 Möck S & Del Vecchio A (2023). Investigation of motor unit behavior in exercise and sports
576 physiology: challenges and perspectives. *Appl Physiol Nutr Metab*; DOI: 10.1139/apnm-
577 2023-0354.

578 Negro F, Muceli S, Castronovo AM, Holobar A & Farina D (2016). Multi-channel intramuscular
579 and surface EMG decomposition by convolutive blind source separation. *J Neural Eng*;
580 DOI: 10.1088/1741-2560/13/2/026027.

581 Oliveira AS & Negro F (2021). Neural control of matched motor units during muscle shortening
582 and lengthening at increasing velocities. *J Appl Physiol* **130,** 1798–1813.

583 Orssatto LBR, Fernandes GL, Blazevich AJ & Trajano GS (2022). Facilitation-inhibition control
584 of motor neuronal persistent inward currents in young and older adults. *J Physiol* **600,**
585 5101–5117.

586 Pearcey GEP, Khurram OU, Beauchamp JA, Negro F & Heckman CJ (2022). Antagonist tendon
587 vibration dampens estimates of persistent inward currents in motor units of the human
588 lower limb. *bioRxiv*2022.08.02.502526.

589 Powers RK, Nardelli P & Cope TC (2008). Estimation of the contribution of intrinsic currents to

motoneuron firing based on paired motoneuron discharge records in the decerebrate cat. *J Neurophysiol* **100,** 292–303.

Rainoldi A, Melchiorri G & Caruso I (2004). A method for positioning electrodes during surface EMG recordings in lower limb muscles. *J Neurosci Methods* **134,** 37–43.

Rassier DE, MacIntosh BR & Herzog W (1999). Length dependence of active force production in skeletal muscle. *J Appl Physiol* **86,** 1445–1457.

Škarabot J, Beauchamp JA & Pearcey GE (2023). Human motor unit discharge patterns reveal differences in neuromodulatory and inhibitory drive to motoneurons across contraction levels. *bioRxiv*2023.10.16.562612.

Stephenson JL & Maluf KS (2011). Dependence of the paired motor unit analysis on motor unit discharge characteristics in the human tibialis anterior muscle. *J Neurosci Methods* **198,** 84–92.

Thorstensen JR (2022). Persistent inward currents in spinal motoneurones: how can we study them in human participants? *J Physiol* **600,** 3021–3023.

Udina E, D'Amico J, Bergquist AJ & Gorassini MA (2010). Amphetamine increases persistent inward currents in human motoneurons estimated from paired motor-unit activity. *J Neurophysiol* **103,** 1295–1303.

Vandenberk MS & Kalmar JM (2014). An evaluation of paired motor unit estimates of persistent inward current in human motoneurons. *J Neurophysiol* **111,** 1877–1884.

Del Vecchio A, Holobar A, Falla D, Felici F, Enoka RM & Farina D (2020). Tutorial: Analysis of motor unit discharge characteristics from high-density surface EMG signals. *J Electromyogr Kinesiol*; DOI: 10.1016/j.jelekin.2020.102426.

Villalba MM, Fujita RA, Stoelben KJV, Silva NR dos S & Gomes MM (2024). Effects of Co-Contraction Training on Neuromuscular Outcomes of Elbow Flexors and Extensors: A Systematic Review and Meta-Analysis. *Int J Strength Cond*; DOI: 10.47206/IJSC.V4I1.243.

Wei K, Glaser JI, Deng L, Thompson CK, Stevenson IH, Wang Q, Hornby TG, Heckman CJ & Kording KP (2014). Serotonin affects movement gain control in the spinal cord. *J Neurosci* **34,** 12690–12700.

Wickham H, Chang W, Henry L, Pedersen TL, Takahashi K WC & Woo K, Yutani H, Dunnington D Rs (2023). ggplot2: create elegant data visualisations using the grammar of graphics (Online). Available at: https://cran.r-project.org/package=ggplot2.

Zbidi S, Zinoubi B, Hammouda O, Vandewalle H, Serrau V & Driss T (2017). Co-contraction training, muscle explosive force and associated electromyography activity. *J Sports Med Phys Fitness* **57,** 725–733.